Hindawi
International Journal of Photoenergy
Volume 2019, Article ID 8090817, 8 pages
https://doi.org/10.1155/2019/8090817

Research Article

Simulation Analysis of Various Applications of a Combined Photovoltaic Panel with a Single-Channel Natural Flow Heat Collector

Asliddin Komilov

Physical-Technical Institute of the Academy of Science of Uzbekistan, Chingiz Aytmatov St. 2B, Toshkent, 100084, Uzbekistan

Correspondence should be addressed to Asliddin Komilov; asliddin@rambler.ru

Received 23 August 2019; Accepted 24 October 2019; Published 19 November 2019

Academic Editor: Jegadesan Subbiah

The present article presents simulation results of a combined photovoltaic panel (PV) with natural flow single-channel thermal collector device (PV/T) for different thermal performance modes. The efficiencies of the PV/T and the same size photovoltaic panel are compared. Stress analysis was performed to realize the system's limitation and resistibility to hydrostatic pressure. At different modes of operation, the photovoltaic efficiency was 6-15% higher for PV/T than for PV. The photovoltaic efficiency of PV/T was less influenced by insulation than that of PV, and combined thermal and photovoltaic efficiency was higher in insulated PV/T. Because of the hydrostatic pressure of water, the proposed design PV/T can use only limited existing PV panels which is a big disadvantage compared to other designs.

1. Introduction

The main concept of the PV/T system is to provide a photovoltaic converter (PV panel) with heat removal by means of a liquid (water) or gas (air) heat carrier. It is a single device in which photovoltaic efficiency is increased by lowering PV temperature, and the solar energy that does not take part in photovoltaic conversion is converted into thermal energy. Previews literature shows that the application potential of PV/T is already acknowledged through many studies [1, 2]. They have low operating costs and expected service of 20-30 years, very suitable for building integration [3, 4] and drying applications [5]. Market potential of PV/T is higher because it has a higher total conversion rate of solar energy compared to photovoltaic and solar thermal systems separately [6, 7].

However, the reliability and cost of the product [8] and costs of recoupment, production, and installation [3] are still issues to be solved in order for PV/T to be successfully implemented [2].

One of the promising concepts is the single-channel PV/T, which requires less materials, so it is cheaper. Maximal heat exchange is insured by a large heat exchange surface from direct contact of water with the back surface of the photovoltaic converter.

The revision of works concerning PV/T devices shows that most of the latest reviews [2–4, 8–11] refer to a single theoretical study [12] of single-channel PV/T device, which concluded that "the channel-below-transparent-PV design gives the best efficiency; but since the annual efficiency of the IV-on-sheet-and-tube design in a solar heating system was only 2% worse, and is easier to manufacture, this design was considered to be a good alternative." Another study [13] used a similar collector design coupling with linear Fresnel concentrator because, according to the results shown in [12], "it gives one of the best ratios of electrical to thermal efficiencies in high irradiance conditions." Another article [14] is limited to an experimental study of a channel collector PV/T device prototype with a 1.29×0.33 m surface. Authors of a later work [15] also consider such design, but the existing information, on channel PV/T devices, is not enough to evaluate the full potential of this concept. Many related formulae were used in [16], but the concept itself has optical disadvantages and the design limits are not discussed. In

addition, the authors omit the influence of glass cover reflectivity, temperature gradient of the PV structure, and bottom side insulation.

This article presents photovoltaic performance and overall valuation of the proposed PV/T and highlights the advantages and disadvantages of this particular construction for various applications. The system uses natural flow, which is more cost effective and has reduced hydrostatic pressure on PV and collector construction. Analyses were executed using experiments and modeling in order to realize the system's limitations in performance, construction, and geometry.

2. Methodology

2.1. Performance Model. Simulation of PV/T in realistic conditions was done using a developed model, where the temperature gradient along vertical axes on the PV surface and of the water inside the collector is linear, and no temperature gradient along horizontal axes for both in any direction. System energy balance:

$$Q_{\mathrm{I}} - U_{\mathrm{f}} - Q_{\mathrm{el}} - Q_{\mathrm{pv}} - Q_{\mathrm{hw}} = 0, \tag{1}$$

which can be schematically represented as follows:

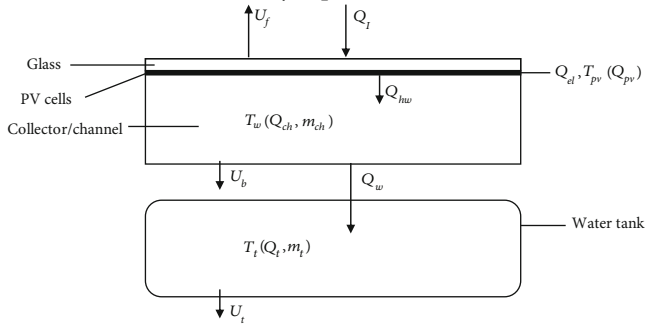

Different from amorphous silicon, temperature coefficient of a crystalline silicon solar cell is not temperature dependent [17]. So constant temperature coefficient can be used to calculate the photovoltaic performance, which is taken as $C_T = -0.0054$.

$$\eta_{\mathrm{el}} = \eta_{\mathrm{ref}} + C_T\left(T_{\mathrm{pv}} - T_{\mathrm{ref}}\right). \tag{2}$$

$$Q_{\mathrm{el}} = \alpha\tau Q_I \eta_{\mathrm{el}}. \tag{3}$$

Energy balance of the collector part is

$$Q_{\mathrm{hw}} - U_{\mathrm{b}} - Q_{\mathrm{ch}} - Q_{\mathrm{w}} = 0. \tag{4}$$

Energy balance of the water tank is

$$Q_{\mathrm{w}} - U_{\mathrm{t}} - Q_{\mathrm{t}} = 0. \tag{5}$$

The model was described in detail, and its outputs were compared with the indoor and outdoor experimental measurements in the earlier work [18]. The volume of the water inside the channel will change according to its geometry. The water tank is a horizontal cylinder, located just above the PV/T, and has a length equal to the top side of PV/T. The diameter of the cylinder will adjust according to the given total volume of the water in the system, without the part inside the channel. The model does not take into consideration the inlet and outlet water tubes connecting the water tank and the channel.

To evaluate the quality of thermal performance, the exergy efficiency of heat production is calculated using the following equation:

$$\eta_{\mathrm{thEx}} = \left(1 - \frac{T_a}{T_2}\right) * \eta_{\mathrm{th}}, \tag{6}$$

where $T_2 = (m_{\mathrm{ch}}/(m_{\mathrm{ch}} + m_{\mathrm{t}}))\mathrm{Tw} + (m_{\mathrm{t}}/(m_{\mathrm{ch}} + m_{\mathrm{t}}))\mathrm{Tt}$ (m_{ch} and m_{t} are the mass of the water in the collector and water tank, accordingly), $\eta_{\mathrm{th}} = Q_{\mathrm{t}}/(I * A * \mathrm{dt})$ (A: area of the PV, dt: exposure time to sunlight I), and the system has the following total efficiency:

$$\eta_{\mathrm{total}} = \eta_{\mathrm{el}} + \eta_{\mathrm{thEx}}. \tag{7}$$

2.2. Material Durability Model. It was noticed during the tests that the collector channel bottom was deformed (bent) under the hydrostatic pressure of water. The manufacturer assured that the bending is in the range of the load safety margin. Nevertheless, bending of the collector bottom above 1 mm could potentially cause cracks in the adhesive between the PV and collector, which, in the long term, results in water leakage. Stability of the glass of the PV converter against hydrostatic pressure is also important, because excessive bending can destroy solar cells. For this reason, the bending properties of galvanized iron sheets and glass of different thicknesses were modeled, using SolidWorks software. The main purpose was to identify minimum thickness that can be used for construction, because the thickness of the material increases both weight and cost. Use of corrugated wave-shaped construction of the collector bottom was found to be a better option [19]. In the present work, the bending of the collector bottom of a bowed shape was analyzed, since it is simpler from application point of view compared to a corrugated shape.

Hydrostatic pressure was calculated using the following formula:

$$P_{\mathrm{h}} = h\rho g \cos\alpha. \tag{8}$$

The factor of safety was calculated to evaluate the stability of the construction. For identification of the minimum possible safety factor at the maximum possible hydrostatic pressure and bending, the formula (8) is used at $\alpha = 0$. The weight of the construction is calculated using the estimated material thickness. A detailed description of the model is given in [19]. The size of the experimental PV/T device was chosen to be 0.2 m^2 to provide resistance to hydrostatic pressure, since a commercial photovoltaic panel would be used that was not designed for this purpose.

Hydrostatic pressure from flow is insignificant because the cross sections of water inlet and outlet are equal and the system uses natural circulation. Load due to the weight of

water is ignored because it is negligible compared to hydrostatic pressure.

2.3. Limits and Conditions. To avoid mistakes in the comparison of the efficiency of the PV panel and the PV/T, the efficiencies are normalized to the reference values, for each device obtained at STC, η/η_{ref}. Normalized electrical efficiencies are calculated for the PV panel and for the PV/T functioning in three different thermal performance conditions (modes):

(i) Mode M1: The water inside the system is not replaced during the day. This is the case for a system which is let alone during the day and heated water is utilized in the evening or during the night time

(ii) Mode M2: The water inside the system is replaced with 20°C feed water when reaching 40°C. Considering the temperature dependence of the photovoltaic efficiency, this mode gives an insight to plausibility of such system to be used for producing "useful" (pre)heated water of a certain temperature, which can be used for example in hot water supply, space heating, drying, or else

(iii) Mode M3: The inlet water temperature is kept constantly equal to the ambient temperature. This mode corresponds to the task when the temperature of the PV is lowered using ambient temperature. In reality, this can be achieved by circulating water in the system through a radiator, which can be mounted at the back (shade) of the PV/T

Thermal performance was evaluated using the same modes.

System was simulated using calculated values of solar irradiance for two different days of the year:

(i) March 1 (D1) and daily lowest and highest temperature of 0°C and 20°C, respectively. This date was chosen to minimize uncertainty due to temperatures below zero, since the model does not consider the phase change of the water

(ii) August 1 (D2) and daily lowest and highest temperature of 20°C and 40°C, respectively, corresponds to the days of similar temperature range in given location

3. Results and Discussion

3.1. Real-Time Data. During the experiments, the PV panel temperature reached values about 90°C. This does not happen regularly, but it shows the extremity of the working conditions of PV panels in real conditions. The measured daily dynamics of the performances of the PV panel and PV/T in mode M1 are presented in Figure 1. The maximum temperature of the day about 49°C, and irradiance is around 900 W/m^2. The maximum surface temperature for this day was 91°C for the PV panel and 74°C for the PV/T system.

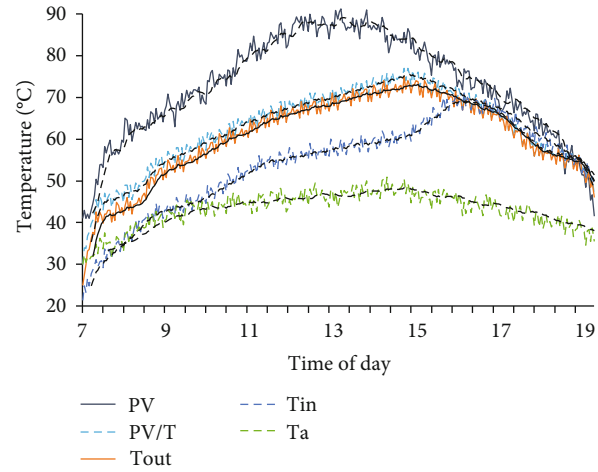

Figure 1: Measured daily dynamics of temperatures and their trend lines (21 July 2018).

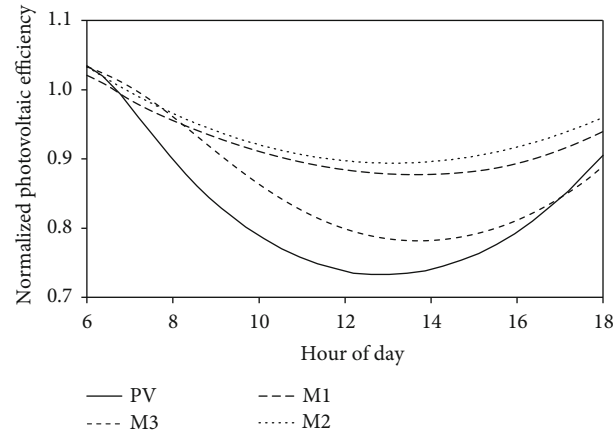

Figure 2: Daily dynamics of normalized photovoltaic efficiencies (21 June 2018).

On average, the surface temperature of the PV/T system was 13°C lower than that of the surface temperature of the PV panel, and a time lag of 5 hours between temperature maximums. Higher surface temperatures are reached at high irradiance hours for the PV panel and high ambient temperature hours for the PV/T. Thus, there are two mechanisms that provide increased power generation in PV/T: (1) reducing the temperature of the photoelectric converter in general and (2) providing a lower temperature particularly in high-radiation hours.

Figure 2 shows the daily dynamics of normalized efficiencies of the PV panel and the PV/T in different modes. The data is based on measured values for the PV panel and the PV/T in M1 mode. Data for other modes were calculated using corresponding values of normalized efficiencies for different temperatures at M1 as reference. For clarity of the figure, polynomial trend lines of the data are presented.

Figure 2 demonstrates that

(i) Real-time photovoltaic efficiency may decrease by more than 25% during the day compared to its nominal value

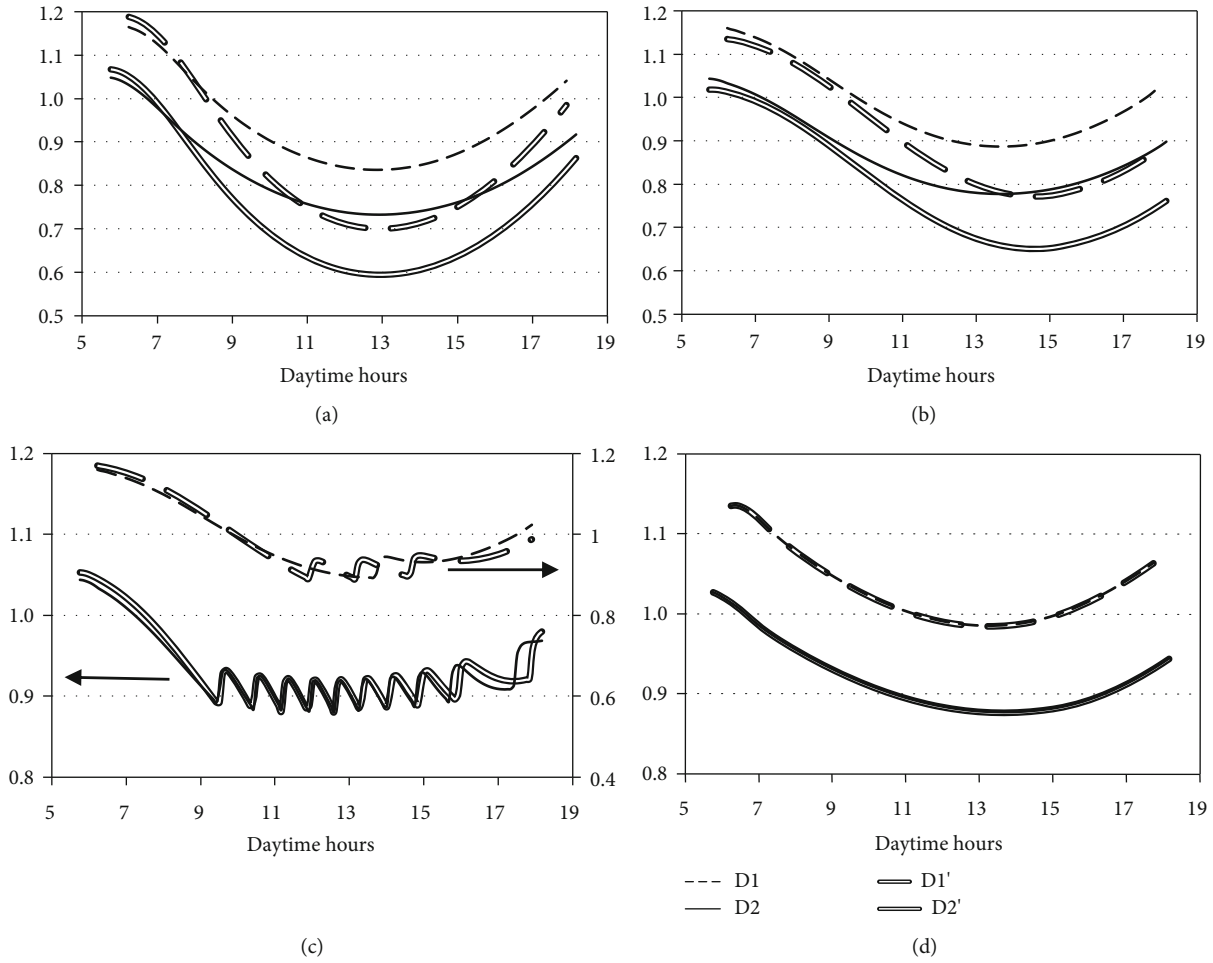

Figure 3: Daily dynamics of normalized photovoltaic efficiencies: (a) PV panel, PV/T; (b) M1, (c) M2, (d) M3; $'$ means that the device is insulated.

(ii) Up to 10% efficiency degradation of PV panel due to the temperature can be prevented if it is used in PV/T even in M1 mode, i.e., without replacing the water in the system during the day. At the end of the day, the photovoltaic efficiency of PV/T is smaller than that of PV, because its temperature is higher due to the higher temperature of the water in the system. At this point, the water in the system will start cooling down if the check valve is not used

(iii) Photovoltaic efficiency of the PV/T during the day was up to 20% higher than that of PV in modes M2 and M3. Photovoltaic efficiency of the PV/T in these two modes are comparable

3.2. Photovoltaic Performance. The daily dynamics of normalized efficiencies of the system in different modes simulated for the cases when the water tank and backside of the collector is with and without insulation. The influence of insulation is of interest since insulation adds cost and weight to the construction. Besides, an insulated system behavior gives insight into the cases of building integration, where the building insulates backside of the collector and the water tank is located inside and insulated from outdoor temperatures.

Photovoltaic efficiencies of PV/T in modes M1 (Figure 3(b)) differ when used with or without insulation that is similar to PV panel (Figure 3(a)). However, for the PV/T in modes M2 and M3 (Figures 3(c) and 3(d), respectively), photovoltaic efficiencies are almost the same when used with or without insulation.

Due to the lowered temperature, similar for March (D1) and August (D2), the photovoltaic efficiency of the device is higher than that of a PV panel even in M1 mode (Figure 3(b)) around 6%; in mode M2 (Figure 3(c)), the photovoltaic efficiency of PV/T is higher over 15%, and in mode M3 (Figure 3(d)), the system's photovoltaic efficiency is around 15% higher than that of PV.

If the PV panel is closely fixed to a surface (for example, a wall or a roof), this serves as an insulation that increases its temperature and can decrease the PV efficiency by an additional 11% (Figure 3(a)). In case of PV/T, the insulation additionally reduced the photovoltaic efficiency by 8% in the M1 mode (Figure 3(b)); effect of insulation on photovoltaic efficiency in other modes was insignificant (Figures 3(c) and 3(d)).

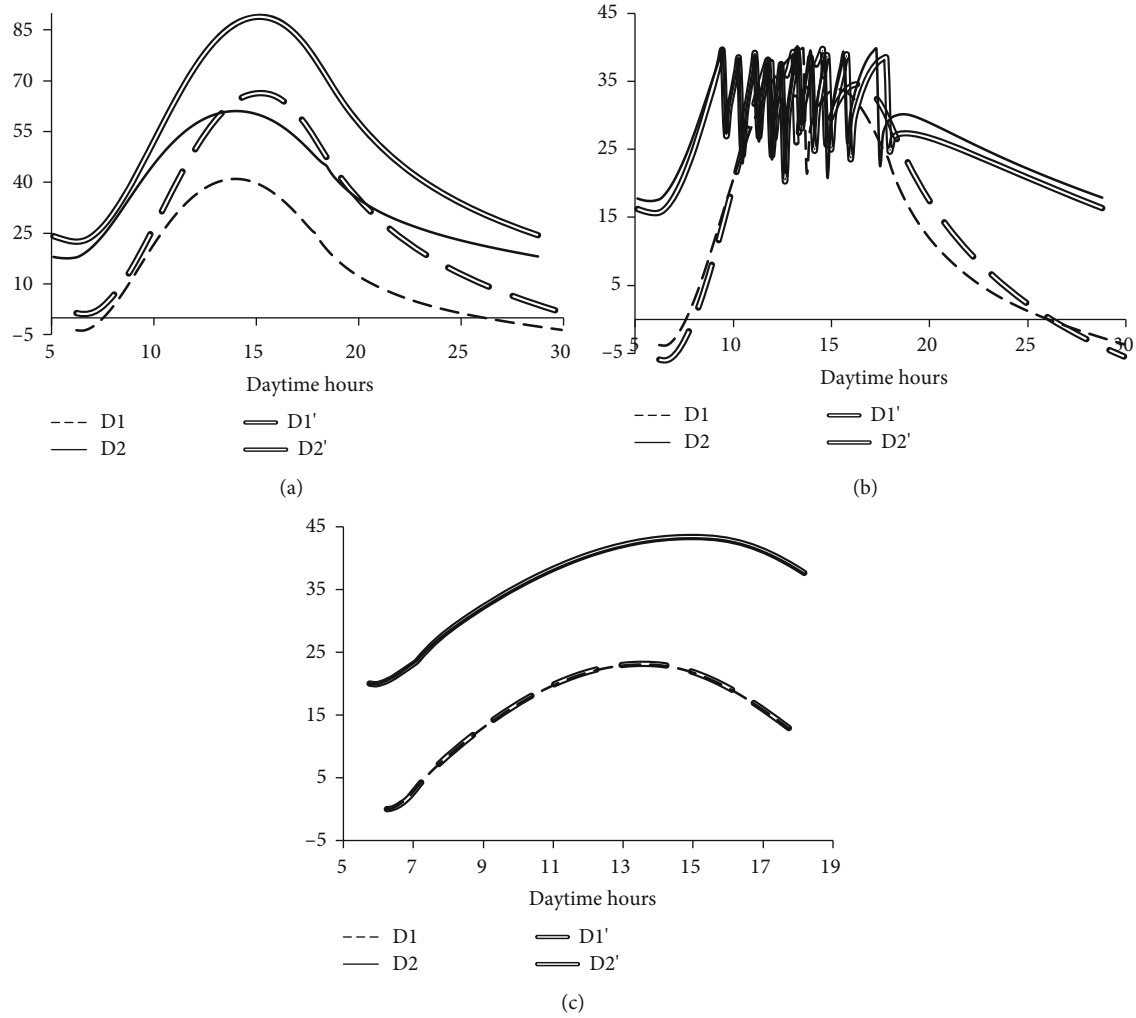

Figure 4: Calculated daily dynamics of water temperature: (a) M1, (b) M2, (c) M3; $'$ means that the device is insulated.

3.3. Thermal Performance. Thermal performance of the device in different modes is demonstrated through the water temperature dynamics during the day (Figure 4). The results presented in Figure 4 are calculated for ideal conditions: ideal insolation at clear sky and zero wind speed thus represents the device performance at its best.

The results in Figures 4(a) and 4(b) show that the PV/T device keeps the properties of a solar collector and can heat the water to higher temperatures (Figure 4(a)) or to produce water of a certain temperature (Figure 4(b)). Figure 4(c) demonstrates that the system has an effective flow rate that does not allow the water to heat up a lot higher than the ambient temperature (mode M3).

3.4. Total Efficiency Evaluation. One of the main features of the PV/T system is its thermal energy, which is generated in addition to the electrical energy generated by its photoelectric converter. The amount of the exergy efficiency of the system demonstrates the amount of additional thermal energy produced by the system that is qualitatively comparable to electricity. The exergy efficiency of heat production in insulated PV/T is bigger due to its higher thermal efficiency (Figure 5(a)), and the temperature difference between water and the environment, especially in a cooler day (D1$'$). The exergy efficiency in the M3 mode is comparable in isolated and nonisolated cases and for different seasons due to the small temperature difference (1) for isolated and nonisolated cases (Figure 3(c)) and (2) water and the environment due to the specification of the mode.

Another feature of the PV/T system is the increase in the photovoltaic efficiency due to heat removal from photovoltaic converters. As can be seen in Figure 5(b), the magnitude of the improvement in photovoltaic efficiency ($\eta_{\mathrm{PVT}} - \eta_{\mathrm{PV}}$) (Figure 5(b)) is higher than that of exergy generated by thermal energy (Figure 5(a)). Improvement in photovoltaic efficiency in the case of the insulated system is also higher because insulation decreases PV efficiency more (Figure 5(c)). Consequently, in the case of insulation, the PV/T system has a higher total normalized efficiency compared to PV (Figure 5(c)). In general, total normalized efficiency of the PV/T system is higher in cooler days (Figure 5(c) D1, D$'$). The small exergy efficiency of heat production in M1 (Figure 5(a)) on hot days (D2) is obvious by formula (6), since the outlet water temperature of 40°C is

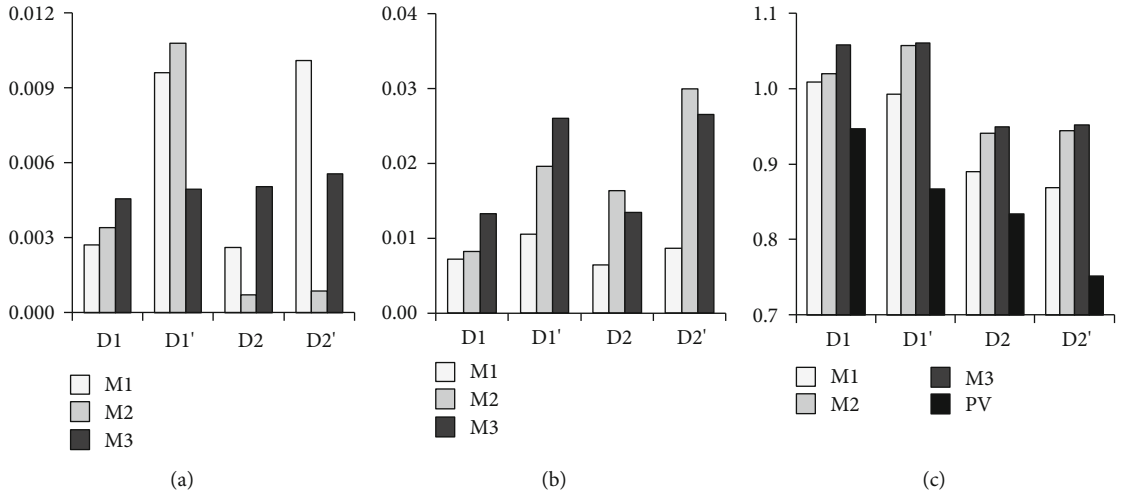

Figure 5: Daily mean values of the exergy efficiency of heat production (a), improvement of photovoltaic efficiency (b), and total normalized efficiency (c) of PV/T in different modes: 1, M1; 2, M2; 3, M3; 4, PV.

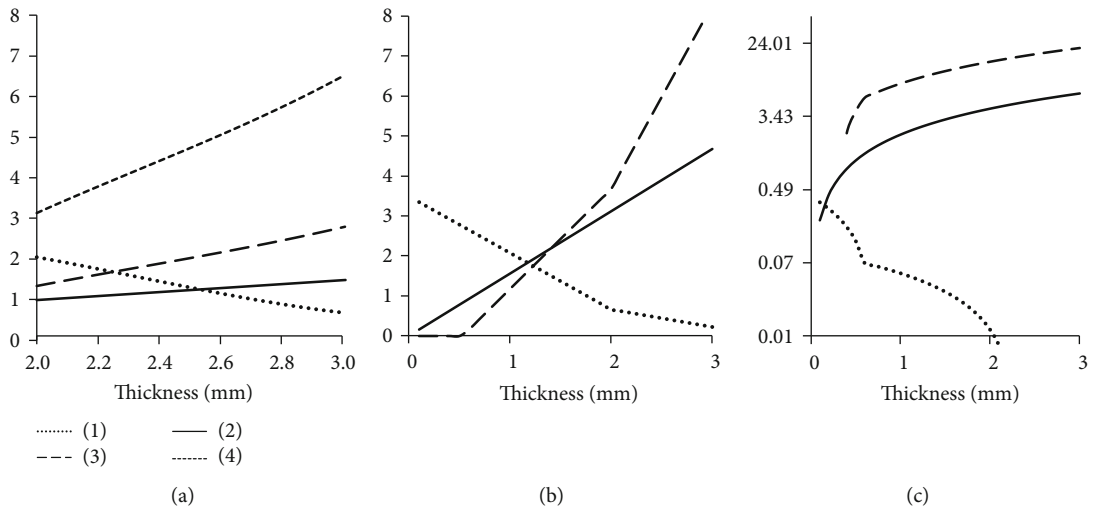

Figure 6: Results of the material durability model: (a) glass; galvanized steel: (b) plain sheet, (c) bowed shape; 1 maximum bending (mm); 2 weight (kg); 3 factor of safety; 4 factor of safety for reinforced glass.

very close to the ambient temperature. For the same reason, the exergy efficiency of heat production in M1 (Figure 5(a)) is high because it always produces water with a higher temperature than the ambient temperature, especially when using insulation.

The amount of daily water utilized in the system is also an important feature and depends on the working mode. The thermal model for the test size device of 0.2 m^2 PV/T will produce water at the same temperature if it uses 10 to 40 liters. Performance in mode M3 is regular if more than 10 liters of water is used. The modeling of the system in mode M2 resulted in maximum daily production of water of 40°C temperature, 93 liters in summer (D2), 38 and 11 liters in a cool day (D1) for insulated and not insulated system accordingly.

3.5. Influence of the Hydrostatic Pressure. Figure 6 shows the results of the material durability model: bending, factor of safety, and weight of glass of different thicknesses. Calculated bowed shape collector bottom had 3 cm bending (Figure 6(c)).

Material durability analysis shows that geometry is very important for this particular PV/T design. The tested size of the device can be produced by using a PV converter since it is made of glass thicker than 2.7 mm, to insure >1 mm bending (Figure 6(a)). The use of reinforced glass is more suitable because its safety factor is more than 2.5 times higher (Figure 6(a)). A plain construction of the collector bottom will add over 3 kg weight to the weight of PV converter, because the sufficient thickness of the metal sheet is over 1.8 mm (Figure 6(b)). The collector bottom can be made thinner in case of BIPV/T, when it will be supported by the facade or roof of the building. Otherwise, the added weight can be reduced below 1 kg if the bowed shape construction of the collector bottom is used (Figure 6(c)). The calculations showed that larger-sized devices of this construction are not plausible due to the added weight. For example, a similar analysis of glass for a device sized 1×1 m showed that the

tolerable thickness is over 10 mm and the weight is more than 25 kg. Calculations show that using PV/T placed in width will decrease hydrostatic pressure.

4. Conclusions

The surface temperature of the photovoltaic panel up to 91°C was recorded during the experiments; the maximum PV/T surface temperature on the same day was 74°C. The maximum temperature of the PV panel is reached at the maximum irradiance, resulting in maximum losses in daily production. The maximum temperature of the PV/T is reached at the maximum ambient temperature hours, which leads to an increased electricity generation by lowering the temperature of the photoelectric converter and providing higher photovoltaic efficiency especially during high radiation hours.

Real-time photoelectric efficiency has been shown to decrease by more than 25% during the day compared to its nominal value. At least 10% efficiency degradation was avoided in the PV panel used in the PV/T system, and up to 20% efficiency degradation prevented when the PV panel is used in the PV/T system with a limited/controlled water temperature.

The simulated performance characteristics of the proposed single-channel PV/T for insulated and not insulated conditions in three different application modes on two different days of the year were presented. The PV/T photovoltaic efficiency and the PV module of similar nominal characteristics were compared. Insulation, which may be due to the integration of the PV of the roof or facade, seriously affects its effectiveness, reducing it by about 30% during a colder day with a maximum ambient temperature of 20°C and about 40% on a hot day with a maximum ambient temperature 40°C. In the case of the PV/T system, even if it is not used during the day, and heated water is used in the evening or at night, these values are slightly higher than 20% and about 35%, respectively, at the corresponding water temperatures of above 65°C and 85°C, respectively. The minimum real-time efficiencies were approximately 10% lower than the nominal values on both cold and hot days when the PV/T system is used to produce water at a temperature of 40°C. When the generated heat is dumped to the environment to ensure the cooling of the photovoltaic converter, the minimum real-time efficiencies were about 2% on a cold day and about 12% on a hot day, at corresponding water temperatures above 20°C and 40°C, respectively. In both cases, the effect of isolation was negligible; thus, there is no problem of photovoltaic efficiency degradation due to building integration, which is observed for the PV panel. Moreover, the insulated PV/T system produces more heated water in a cool day.

Paradox of PV/T, where thermal production verses electrical production, requires good balance of the two to ensure efficacy. Since thermal energy and electrical energy are not comparable directly, the exergy efficiency of heat production is used. Calculated exergy efficiency of heat production is at least 2 times than the improvement in photovoltaic efficiency in the same mode compared to PV panel. In all modes, the overall normalized PV/T efficiency is higher than the efficiency of the PV panel, especially in cases of insulation, therefore when integrated into a building.

The analysis showed the advantage of a combined photovoltaic panel with a single-channel thermal collector with natural flow in various modes; however, in a system with a larger surface area, the glass of the photovoltaic converter must be thicker to withstand the hydrostatic pressure of water, and this is a big disadvantage compared to other designs. A likely application would be the connection of horizontally located small units, and this, of course, will impede its large-scale use.

Nomenclature

A: Surface area of the device (m^2)
C_T: Temperature coefficient of photovoltaic efficiency (K^{-1})
G: Global solar irradiance (W/m^2)
I_{sc}: Short circuit current (A)
P_h: Hydrostatic pressure (N/m^2)
Q_{el}: Energy converted into electricity (J)
Q_{hw}: Energy transferred from PV convertor into the water in collector channel (J)
Q_{ch}: Energy absorbed by the water volume in collector channel (J)
Q_I: Energy of solar irradiation (J)
Q_{pv}: Energy absorbed by the PV converter (J)
Q_t: Energy absorbed by the water volume in water tank (J)
Q_w: Energy transferred to the water in water tank (J)
T_a: Ambient temperature (°C)
T_{max}: Maximum daily ambient temperature (°C)
T_{min}: Minimum daily ambient temperature (°C)
T_{pv}: PV converter temperature (°C)
T_{ref}: PV converter reference temperature (25°C)
T_t: Temperature of water in the tank bulk (°C)
T_w: Temperature of water in the collector bulk (°C)
ΔT_w: Mean temperature of water in the collector channel bulk (°C)
U_f: Losses from PV converter front surface (J)
U_b: Losses from PV converter back surface (J)
U_t: Losses from water tank surface (J)
V_{oc}: Open-circuit voltage (V)
cp_w: Specific heat capacity of the water, 4181.3 J/(kg*K)
g: Gravity constant, 9.8 m/s^2
h: Height of the device (m)
m_{ch}: Mass of water in the collector channel (kg)
m_t: Mass of water in the water tank (kg)
$\dot{m}$: Mass flow of water through the collector channel (kg/s)
dt: Period of time (s).

Greek Letters

α: Tilt angle of the device plane (°)
η_{ref}: Reference photovoltaic/electrical efficiency (provided by manufacturer)
η_{th}: Thermal efficiency
η_{thEx}: Exergy efficiency of heat production
ρ: Density (kg/m^3)

ϑ_w: Water velocity (m/s)
η_{el}: Photovoltaic/electrical efficiency
$\alpha\tau$: Optical efficiency.

Acronyms

BIPVT: Building integrated PV/T
PV: Photovoltaic device
PV/T: Photovoltaic thermal device
STC: Standard test conditions.

Data Availability

The information and data used in this article is available at corresponding references.

Conflicts of Interest

The author declares that there is no conflict of interest regarding the publication of this paper.

Acknowledgments

This work has been supported by the Ministry of Innovative Development of the Republic of Uzbekistan.

References

[1] V. V. Tyagia, S. C. Kaushika, and S. K. Tyagib, "Advancement in solar photovoltaic/thermal (PV/T) hybrid collector technology," *Renewable and Sustainable Energy Reviews*, vol. 16, no. 3, pp. 1383–1398, 2012.

[2] M. Arif Hasan and K. Sumathy, "Photovoltaic thermal module concepts and their performance analysis: a review," *Renewable and Sustainable Energy Reviews*, vol. 14, no. 7, pp. 1845–1859, 2010.

[3] A. Ibrahim, M. Y. Othman, M. H. Ruslan, S. Mat, and K. Sopian, "Recent advances in flat plate photovoltaic/thermal (PV/T) solar collectors," *Renewable and Sustainable Energy Reviews*, vol. 15, no. 1, pp. 352–365, 2011.

[4] T. Matuska, "Simulation study of building integrated solar liquid PV-T collectors," *International Journal of Photoenergy*, vol. 2012, Article ID 686393, 8 pages, 2012.

[5] R. Daghigha, M. H. Ruslana, and K. Sopiana, "Advances in liquid based photovoltaic/thermal (PV/T) collectors," *Renewable and Sustainable Energy Reviews*, vol. 15, no. 8, pp. 4156–4170, 2011.

[6] X. Zhanga, X. Zhaoa, S. Smitha, J. Xu, and X. Yu, "Review of R&D progress and practical application of the solar photovoltaic/thermal (PV/T) technologies," *Renewable and Sustainable Energy Reviews*, vol. 16, no. 1, pp. 599–617, 2012.

[7] N. R. Chowdhury, "Design and experimental validation of a photovoltaic-thermal (PVT) hybrid collector," *International Journal of Renewable Energy Research*, vol. 4, pp. 1446–1453, 2016.

[8] T. T. Chow, "A review on photovoltaic/thermal hybrid solar technology," *Applied Energy*, vol. 87, no. 2, pp. 365–379, 2010.

[9] M. Bakker, H. A. Zondag, and W. G. J. van Helden, *Demonstration on a dual flow photovoltaic/thermal combi panel*, From PV Technology to Energy Solutions Conference and Exhibition, Rome, Italy, 2002, October 7-11.

[10] M. N. Tursunov, S. Dadamukhamedov, V. P. Kononerov, A. M. Mirzabaev, and O. F. Tukfatullin, "Investigation of parameters of photothermoconverter based on Si solar cells," *Applied Solar Energy*, vol. 44, no. 1, pp. 17–19, 2008.

[11] P. G. Charalambous, G. G. Maidment, S. A. Kalogirou, and K. Yiakoumetti, "Photovoltaic thermal (PV/T) collectors: a review," *Applied Thermal Engineering*, vol. 27, no. 2-3, pp. 275–286, 2007.

[12] H. A. Zondag, D. W. de Vries, W. G. J. van Helden, R. J. C. van Zolingen, and A. A. van Steenhoven, "The yield of different combined PV-thermal collector designs," *Solar Energy*, vol. 74, no. 3, pp. 253–269, 2003.

[13] J. I. Rosell, X. Vallverdú, M. A. Lechón, and M. Ibáñez, "Design and simulation of a low concentrating photovoltaic/thermal system," *Energy Conversion and Management*, vol. 46, no. 18-19, pp. 3034–3046, 2005.

[14] K. Touafek, M. Haddadi, and A. Malek, "Experimental study on a new hybrid photovoltaic thermal collector," *Applied Solar Energy*, vol. 45, no. 3, pp. 181–186, 2009.

[15] S. Y. Wu, C. Chen, and L. Xiao, "Heat transfer characteristics and performance evaluation of water-cooled PV/T system with cooling channel above PV panel," *Renewable Energy*, vol. 125, pp. 936–946, 2018.

[16] M. Salem Ahmed, M. ASA, and H. M. Maghrabie, "Performance evaluation of combined photovoltaic thermal water cooling system for hot climate regions," *Journal of Solar Energy Engineering*, vol. 141, no. 4, article 041010, 2019.

[17] D. Carlson, G. Lin, and G. Ganguly, "Temperature dependence of amorphous silicon solar cell PV parameters," in *Conference Record of the Twenty-Eighth IEEE Photovoltaic Specialists Conference-2000 (Cat. No. 00CH37036)*, Anchorage, AK, USA, September 2000.

[18] A. Komilov, "Improving the design of a photo-converter with a heat sink using mathematical simulation," *Applied Solar Energy*, vol. 47, no. 3, pp. 229–233, 2011.

[19] A. Komilov, "Calculation of the limits of physical dimensions of PV with heat removal," *Applied Solar Energy*, vol. 49, no. 1, pp. 19–21, 2013.